Use of a Six-dimensional Eye-tracker in Corneal Laser Refractive Surgery With the SCHWIND AMARIS TotalTech Laser

Samuel Arba Mosquera, MSc; Maria C. Arbelaez, MD

ABSTRACT

PURPOSE: To evaluate intraoperative six-dimensional (6D) eye movements and postoperative outcomes among aberrated eyes that underwent LASIK treatments with 6D eye-tracking using the SCHWIND AMARIS platform (SCHWIND eye-tech-solutions).

METHODS: Thirty-four patients (58 eyes) were enrolled in the study. Standard examinations and pre- and postoperative wavefront analyses with the Ocular Wavefront Analyzer (SCHWIND eye-tech-solutions) were performed. Treatments were planned using the Custom Ablation Manager and ablations (aspheric ablation [35 eyes] and ocular wavefront [23 eyes]) were performed using the SCHWIND AMARIS TotalTech laser. Laser in situ keratomileusis flaps were cut using the LDV femtosecond laser (Ziemer Group) in all cases. Eye movements were evaluated in terms of cyclotorsion, rolling, and axial movements. Clinical outcomes were evaluated in terms of predictability, refractive outcome, safety, wavefront aberration, and contrast sensitivity.

RESULTS: Registration rate was 100% for cyclotorsion, and 90% for rolling and axial movements. Static cyclotorsion was within ±4° in 69% of eyes. Dynamic cyclotorsion was within ±2° in 72% of eyes. Z-movement was within ±0.5 mm in 69% of eyes. At 3-month follow-up, 70% of eyes were within ±0.25 diopters (D) of emmetropia. Mean defocus was −0.12±0.17 D and astigmatism was 0.15±0.25 D. Corrected distance visual acuity improved in 19% of eyes.

CONCLUSIONS: Laser in situ keratomileusis with active compensation of 6D eye-movements with a 6D eye-tracker using the SCHWIND AMARIS is safe, predictable, and yields excellent outcomes. Refraction and higher order aberrations were reduced to subclinical values postoperatively without applying additional nomograms. [*J Refract Surg*. 2011;xx(x):xxx-xxx.]
doi:10.3928/1081597X-20110120-02

Human eyes have six degrees of freedom to move: X/Y lateral shifts, Z leveling, horizontal/vertical rotations, and cyclotorsion (rotations around the optical axis). These movements have been analyzed since the middle of the 20th century. Laser technology for refractive surgery allows corneal alterations to correct refractive errors[1] more accurately than ever. Ablation profiles are based on the removal of tissue lenticules in the form of sequential laser pulses that ablate a small amount of corneal tissue to compensate for refractive errors. However, the quality of vision can deteriorate significantly under mesopic and low contrast conditions, especially with increased aberrations.[2]

Induction of aberrations, such as spherical aberrations and coma, is related to loss of visual acuity[3] and quality. To balance already existing aberrations, customized treatments were developed that use either wavefront measurements of the whole eye[4] (eg, obtained by Hartmann-Shack wavefront sensors[5]) or corneal topography–derived wavefront analysis.[6,7] Topography-guided,[8] wavefront-driven,[9] wavefront-optimized,[10] asphericity preserving, and Q-factor profiles[11] have been presented as solutions.

Schwiegerling and Snyder[12] measured eye motion in patients undergoing LASIK using a video technique and determined centration and variance of the eye position during surgery. They found a standard deviation >100 µm in eye movements in all eyes.

Taylor et al[13] determined the accuracy of an eye tracking

From Grupo de Investigación de Cirugía Refractiva y Calidad de Visión, Instituto de Oftalmobiología Aplicada, University of Valladolid, Valladolid, Spain (Arba Mosquera); SCHWIND eye-tech-solutions, Kleinostheim, Germany (Arba Mosquera); and Muscat Eye Laser Center, Muscat, Sultanate of Oman (Arbelaez).

Mr Arba Mosquera is an employee of and Dr Arbelaez is a consultant for SCHWIND eye-tech-solutions, Kleinostheim, Germany.

This work was presented at the American Society of Cataract and Refractive Surgery annual meeting; April 9-14, 2010; Boston, Massachusetts.

Correspondence: Samuel Arba Mosquera, MSc, SCHWIND eye-tech-solutions, Mainparkstr 6-10, D-63801 Kleinostheim, Germany. Tel: 49 6021 508 274; E-mail: samuel.arba.mosquera@eye-tech.net

Received: July 12, 2010; Accepted: January 7, 2011

Posted online: February 1, 2011

system designed for laser refractive surgery. The system demonstrated an accuracy of 60 µm for an intact cornea and 100 µm for a cornea with a thin flap.

Bueeler et al[14] investigated the lateral alignment accuracy needed in wavefront-guided refractive surgery to improve the ocular optics to a desired level in a percentage of normally aberrated eyes. To achieve the diffraction limit in 95% of normal eyes with a 7.0-mm pupil, a lateral alignment accuracy of 70 µm or better was required. An accuracy of 200 µm was sufficient to reach the same goal with a 3.0-mm pupil.

Bueeler and Mrochen[15] quantified the parallax error associated with localizing corneal positions by tracking the subjacent entrance pupil center by means of optical ray-tracing in a schematic eye model. They found that tracking error can amount to 30% (or more for eye trackers mounted closer than 500 mm to the eye) of the detected lateral shift. Thus, if the eye tracker registers a lateral shift of the entrance pupil of 200 µm away from the tracking reference axis, the point of interest located on the cornea would essentially be 260 µm away from this reference axis. A laser pulse fired at that moment would be systematically displaced by 60 µm.

Measuring rotation while the patient is sitting upright[16] to when the refractive treatments are performed with the patient supine may lead to ocular cyclotorsion,[17,18] resulting in mismatching of the applied versus the intended profiles.[19,20] Some equipment has facilitated measurement of and potential compensation for static cyclotorsion occurring when the patient moves from upright to the supine position during the procedure,[21] thus quantifying the cyclorotation occurring between wavefront measurement and laser refractive surgery[22] and compensating for it.[23-25] Further measuring and compensating ocular cyclotorsion during refractive treatments with the patient supine may reduce optical "noise" of the applied versus the intended profiles.[26-28]

Recently, many studies have discussed the methodologies and implications of ocular cyclotorsion, but not many reports pay attention to the rolling and axial movements of the eye. In the current study, we evaluated the intraoperative six-dimensional (6D) eye movements and postoperative outcomes among aberrated eyes that underwent LASIK treatments with 6D eye-tracking using the SCHWIND AMARIS platform (SCHWIND eye-tech-solutions, Kleinostheim, Germany).

PATIENTS AND METHODS

For this prospective study, eyes were divided into aspheric ablation[29] and ocular wavefront[30] groups. Enrollment criteria for the aspheric ablation group were astigmatism ⩾1.00 diopter (D)[20,31] at the corneal plane with root-mean-square (RMS) of the higher order aberration (HOA) <0.38 D[32] (~0.5 µm at 6-mm diameter). Enrollment criterion for the ocular wavefront group was RMS of HOA >0.38 D[20,32] (~0.5 µm at 6-mm diameter) irrespective of the astigmatism magnitude. In total, 58 eyes (35 in the aspheric ablation group and 23 in the corneal wavefront group) of 34 patients were enrolled.

Surgical Technique

All surgeries were performed by one surgeon (M.C.A.). For corneal and conjunctival anesthesia, two drops of proparacaine HCl 0.5% (Aurocaine; Aurolab, Madurai, India) were instilled three times before moving the patient to the operating room. All flaps were created using a LDV femtosecond laser (Ziemer Group, Port, Switzerland) with superior hinges, 110-µm attempted flap thickness, and 9.0- or 9.5-mm nominal flap diameter. A 9-mm marker was used to guide centration and to objectively measure the amount of applanation to achieve better flaps in terms of centration and size. Online pachymetry by means of the integrated optical coherence pachymeter[33] (Heidelberg Engineering, Heidelberg, Germany) was performed to measure stromal bed thickness before and after flap lift. After lifting the flap, ablation was performed preserving flap edges, hinge, and interface of the flap disk from being ablated. Contact lens was applied at the end of surgery (Biomedics 55 evolution; Ocular Sciences, Cooper Vision, Hamble, United Kingdom) in eyes with achieved flap thickness <110 µm. A 6.3-mm central fully corrected ablation zone was used in all eyes with a variable transition size automatically provided by the laser related to the planned refractive correction (6.5 to 8.8 mm). Ablation was performed using the AMARIS excimer laser.[34]

Lateral Movement Tracking During Ablation

A pupil-registration module is included in the eye-tracker subsystem, in which the first pupil image obtained prior to starting the ablation is used as a reference and its location in reference to the limbus is used for further eye-tracker images to determine the pupil center shift compensation.

Eye Rolling Tracking During Ablation

A scleral registration module is included in the eye-tracker subsystem, in which the first few scleral-tracker images obtained when starting the ablation are used as references (natural rolling) and compared to any further scleral-tracker image to determine eye rolling.

Static Cyclotorsion Tracking Between Upright And Supine Positions

An eye registration module is included in the eye-tracker subsystem, in which the diagnosis image (ie, the

corneal image acquired during the measurement of ocular wavefront) is used as a reference and compared to an eye-tracker image obtained prior to starting the ablation to determine the static cyclotorsion component.

Dynamic Cyclotorsion Tracking During Ablation

An eye registration module is included in the eye-tracker subsystem, in which the first eye-tracker image obtained prior to starting the ablation is used as a reference and compared to any further eye-tracker image to determine the dynamic cyclotorsion component.

Axial Displacements During Ablation

A scleral registration module is included in the eye-tracker subsystem, in which the first few scleral-tracker images obtained prior to starting the ablation are used as references (natural level) and compared to any further scleral-tracker image to determine the axial displacements.

Analyses

The reported values are the crude eye movements as measured by the eye tracker and not the direct numerical compensation applied by the system. Moreover, there is no eye-tracker lock-on for the AMARIS system. A 6D registration of the eye during treatment is attempted instead of six different one-dimensional registrations. For this reason, theoretically no over- or undercompensation occurs from the separate effects of two isolated eye movements.

Registration Metrics

The rate of successful registration was calculated for eye rolling, static cyclotorsion component, dynamic cyclotorsion component, and axial displacement values as:

$$(1)\quad EyeRegistrationRate\ (\%) = \frac{RegisteredEyes}{TotalEyes} \cdot 100$$

Mean values, standard deviation, and minimum and maximum values were computed for eye rolling, static cyclotorsion, dynamic cyclotorsion, and axial displacement. These measurements are expressed as percent of treatments.

The difference between the maximum and minimum eye rolling, dynamic cyclotorsion, and axial displacement values for each eye was taken as a metric of the movement range. Mean values, standard deviation, minimum and maximum values were computed for the movement ranges. These measurements are expressed as percent of treatments.

Refractive and Visual Metrics

Refractive outcome, predictability of the astigmatism, safety (corrected distance visual acuity), and change in aberrations were analyzed separately by groups (aspheric ablation and ocular wavefront).

RESULTS

Figure 1 shows the 6D movements of a cooperative patient, whereas Figure 2 shows the 6D movements of an uncooperative patient. Cooperative refers to smooth, regular eye movement observed a posteriori, and uncooperative refers to erratic, irregular patterns of eye movement.

Eye Positions During Ablation

Lateral Eye Positions. Mean pupil center shift compensation was −11±81 µm (range: −172 to +187 µm) for the horizontal axis and −140±158 µm (range: −470 to 77 µm) for the vertical axis (Fig 3). Seventy-nine percent of mean pupil center shift compensation measurements were within 100 µm for the horizontal axis and 48% for the vertical axis (Fig 4).

Eye Rolling. The rate of successful registration for eye rolling was 90% (52/58 successful eye rolling registrations) in this study.

Mean eye rolling was 2±3° (range: −4° to 7°) for the horizontal axis and −3±3° (range: −7° to 1°) for the vertical axis (see Fig 3). Seventy-eight percent of mean eye rolling measurements were within 5° for the horizontal axis and 70% for the vertical axis (see Fig 4).

Static Cyclotorsion Between Upright and Supine Positions. The rate of successful registration for static cyclotorsion was 100% (58/58 successful static cyclotorsion registrations) in this study. Mean static cyclotorsion from upright to supine was 1±4° (range: −6° to 7°) (see Fig 3). Eighty-three percent of static cyclotorsion measurements were within 5° (see Fig 4).

Axial Location. The rate of successful registration for axial displacement was 90% (52/58 successful eye rolling registrations). Mean axial displacement was −295±455 µm (range: −1129 to 404 µm) (see Fig 3). Sixty-seven percent of mean axial displacement measurements were within 500 µm (see Fig 4). Mean axial displacement values were >1 mm in 10% of measurements (see Fig 4).

Eye Movements During Ablation

Lateral Eye Movements. Mean pupil center shift compensation range during treatment was 549±188 µm (range: 256 to 928 µm) for the horizontal axis and 781±356 µm (range: 356 to 1664 µm) for the vertical axis (Fig 5). For the horizontal axis, 55% of pupil center shift compensation ranges were within 500 µm and 24% for the vertical axis (Fig 6). For the vertical axis, 21% of pupil center shift compensation ranges were >1 mm (see Fig 6).

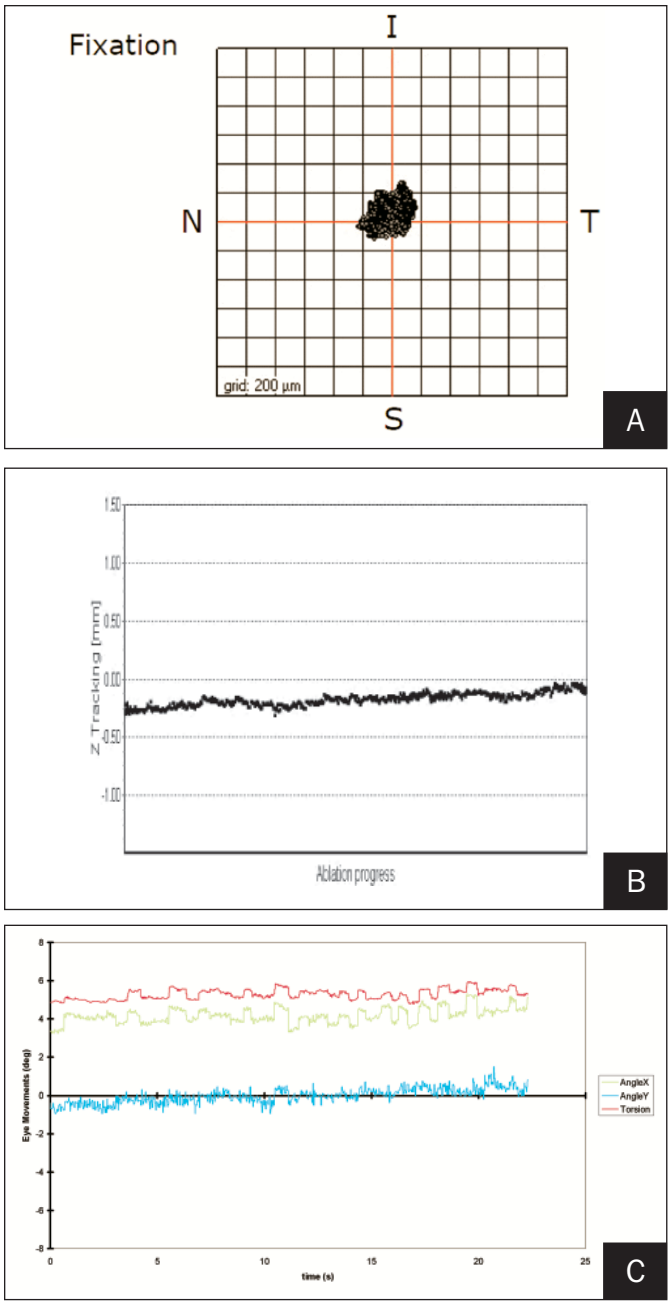

Figure 1. Six-dimensional eye movements of a cooperative patient. **A)** Fixation display depicting the pupil positions detected during the course of treatment (I = inferior, N = nasal, S = superior, T = temporal). **B)** Z-tracking display depicting the axial displacements of the sclera detected during the course of treatment. **C)** Angular display depicting the rolling and torsion movements of the eye detected during the course of treatment. AngleX = horizontal rolling (°), AngleY = vertical rolling (°)

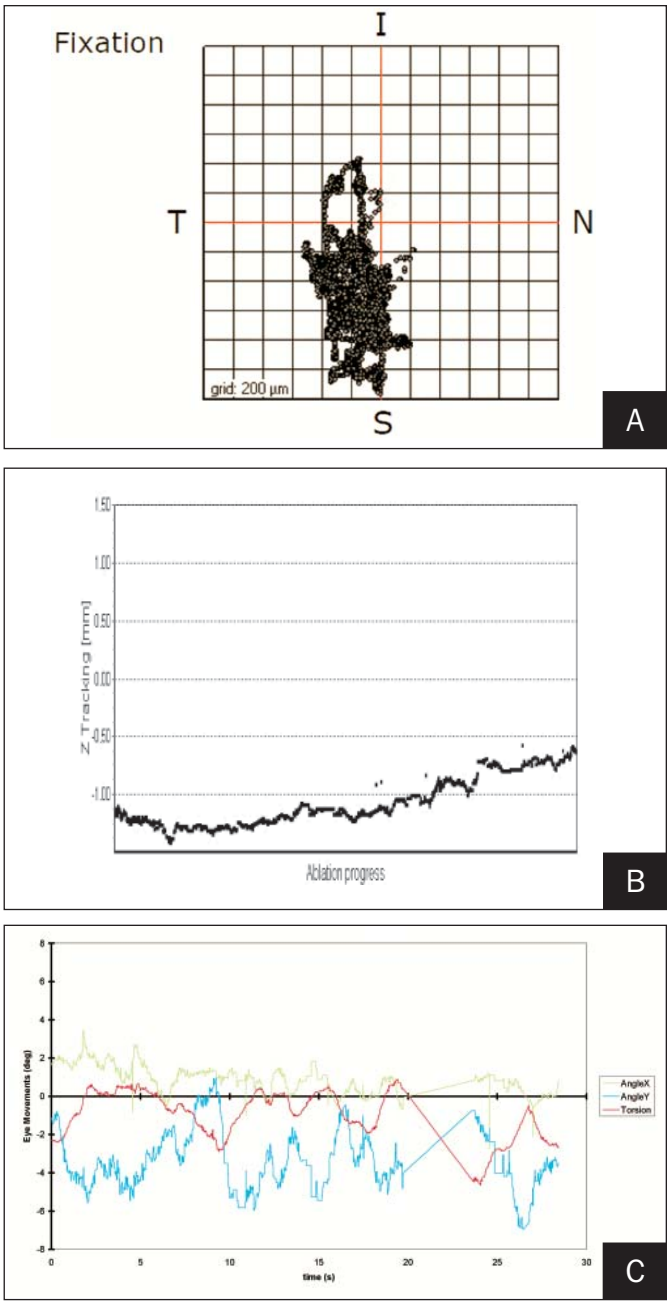

Figure 2. Six-dimensional eye movements of an uncooperative patient. **A)** Fixation display depicting the pupil positions detected during the course of treatment (I = inferior, N = nasal, S = superior, T = temporal). **B)** Z-tracking display depicting the axial displacements of the sclera detected during the course of treatment. **C)** Angular display depicting the rolling and torsion movements of the eye detected during the course of treatment. AngleX = horizontal rolling (°), AngleY = vertical rolling (°)

Eye Rolling Movements. Mean eye rolling range during treatment was 4±2° (range: 1° to 9°) for the horizontal axis and 5±2° (range: 1° to 8°) for the vertical axis (see Fig 5). For the horizontal axis, 78% of eye rolling ranges were within 5° and 67% for the vertical axis (see Fig 6). For the horizontal axis, 3% of eye rolling ranges were >8° (see Fig 6).

Dynamic Cyclotorsion During Ablation. The rate of successful registration for dynamic cyclotorsion was 100% (58/58 successful dynamic cyclotorsion registrations). Mean dynamic cyclotorsion during treatment was 1±1° (range: −1° to 2°). Eighty-six percent of dynamic cyclotorsion measurements were within 1° of cyclotorsion.

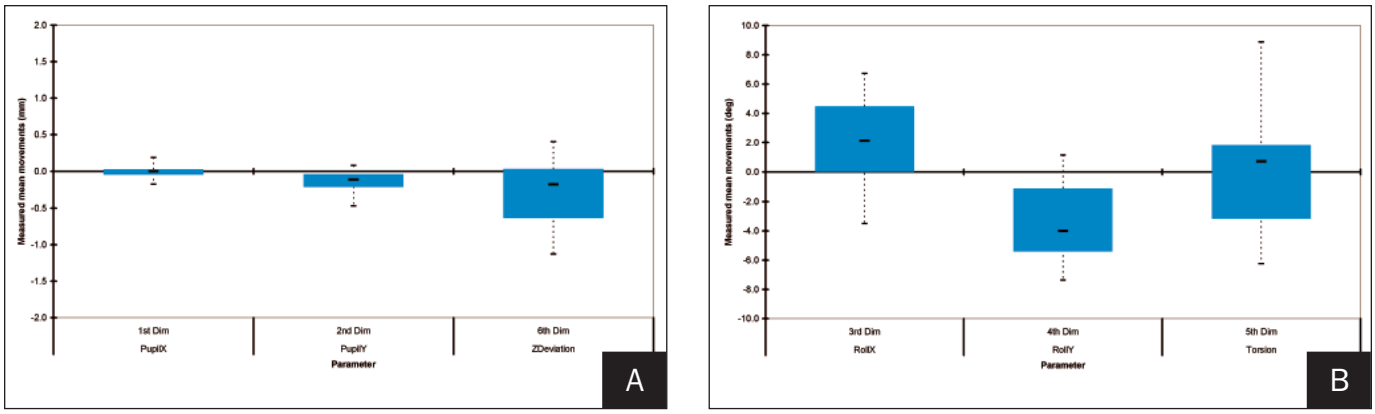

Figure 3. Measured eye positions. **A)** Linear movements (lateral and axial displacements) (PupilX = horizontal lateral shift, PupilY = vertical lateral shift, ZDeviation = axial displacement). **B)** Angular movements (rolling and torsion movements) (RollX = horizontal rolling, RollY = vertical rolling).

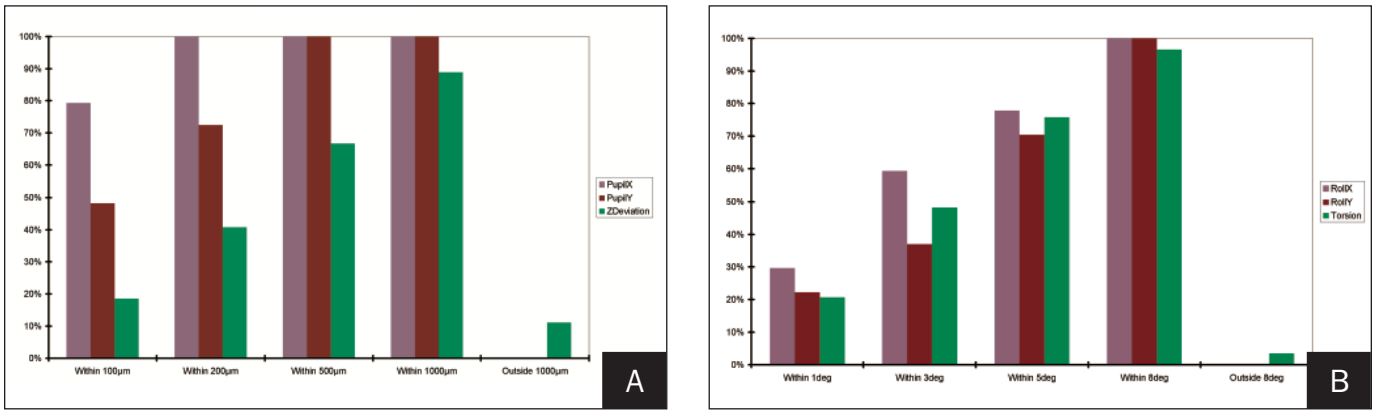

Figure 4. Histogram of the mean eye positions. **A)** Linear movements (lateral and axial displacements) (PupilX = horizontal lateral shift, PupilY = vertical lateral shift, ZDeviation = axial displacement). **B)** Angular movements (rolling and torsion movements) (RollX = horizontal rolling, RollY = vertical rolling).

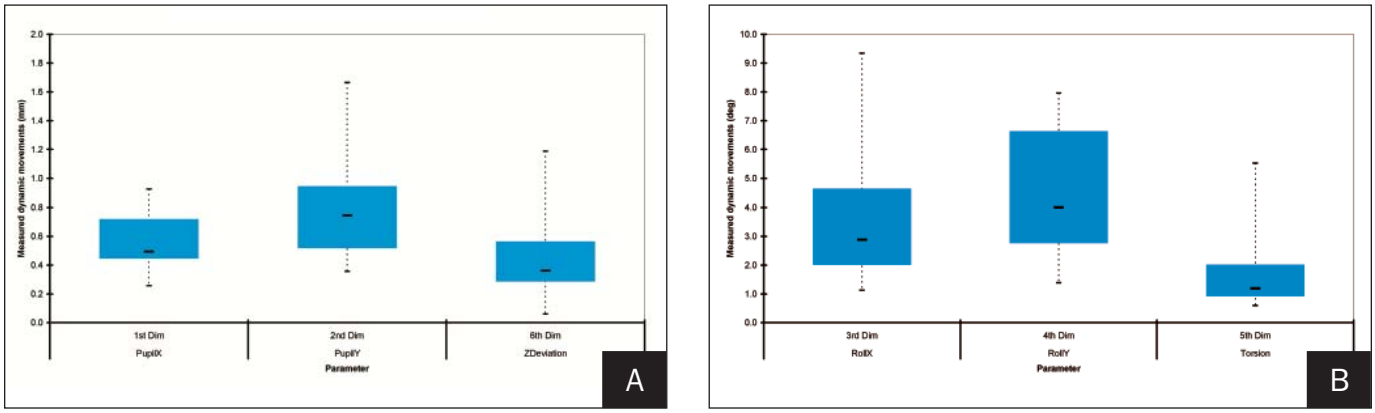

Figure 5. Measured ranges for eye movements. **A)** Linear movements (lateral and axial displacements) (PupilX = horizontal lateral shift, PupilY = vertical lateral shift, ZDeviation = axial displacement). **B)** Angular movements (rolling and torsion movements) (RollX = horizontal rolling, RollY = vertical rolling).

Mean dynamic cyclotorsion range during treatment was 2±1° (range: 1° to 6°) (see Fig 5). Dynamic cyclotorsion amplitudes were within 3° in 83% of eyes (see Fig 6).

Axial Eye Movements. Mean axial displacement during treatment was 460±271 µm (range: 60 to 1188 µm) (see Fig 5). Sixty-seven percent of axial displacement ranges were within 500 µm (see Fig 6). Three percent of axial displacement ranges were >1 mm (see Fig 6).

Manifest Refraction

Mean preoperative spherical equivalent refraction was −3.03±1.47 D (range: −6.25 to −0.50 D) for the aspheric ablation group and −1.51±0.73 D (range: −3.25 to −0.25 D)

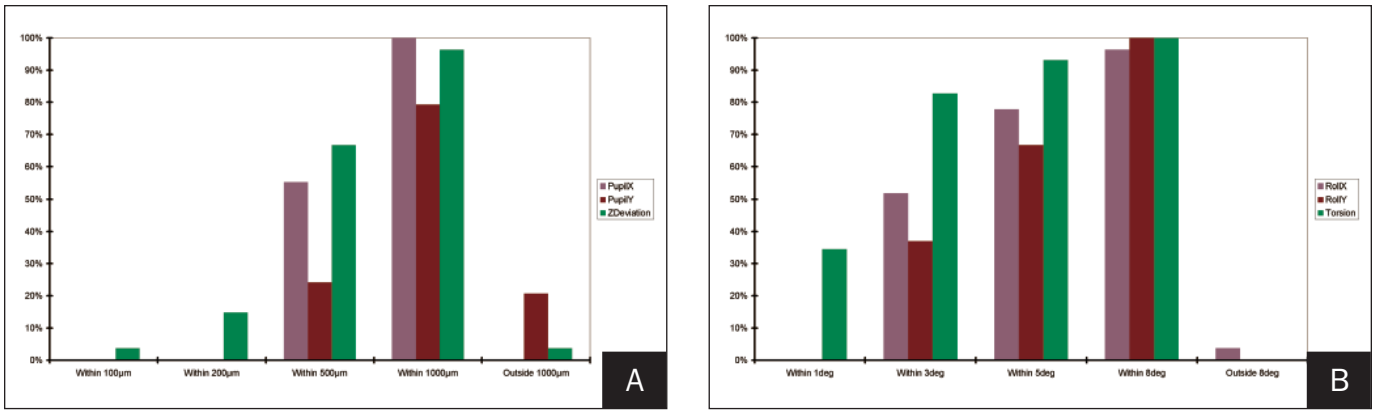

Figure 6. Histogram of the ranges of eye movements. **A)** Linear movements (lateral and axial displacements) (PupilX = horizontal lateral shift, PupilY = vertical lateral shift, ZDeviation = axial displacement). **B)** Angular movements (rolling and torsion movements). (RollX = horizontal rolling, RollY = vertical rolling).

TABLE

Demographics of Patients Who Underwent LASIK With 6D Eye-tracking Using the SCHWIND AMARIS

	Group	
Demographic	**Aspheric Ablation**	**Ocular Wavefront**
No. of eyes	35	23
Age (y)	33 (19 to 49)	35 (22 to 52)
Sex (F/M) (%)	54/46	61/39
Eye (Right/left) (%)	51/49	48/52
Preoperative SEq (D)	−3.03±1.47 (−6.25 to −0.50)	−1.51±0.73 (−3.25 to −0.25)
Preoperative astigmatism (D)	2.03±0.56 (1.50 to 3.50)	0.80±0.39 (0.00 to 3.50)
Preoperative RMS(HOA) at 6-mm (µm)	0.33±0.15 (0.09 to 0.87)	0.53±0.13 (0.34 to 0.98)
Postoperative SEq (D)	−0.13±0.18 (−0.50 to +0.25)	−0.12±0.17 (−0.50 to +0.25)
Postoperative astigmatism (D)	0.15±0.25 (0.00 to 0.75)	0.15±0.25 (0.00 to 0.75)
Postoperative RMS(HOA) at 6-mm (µm)	0.34±0.14 (0.15 to 0.62)	0.35±0.18 (0.10 to 0.89)

SEq = spherical equivalent refraction, RMS = root-mean-square, HOA = higher order aberration
Values represented as mean±standard deviation (range).

for the ocular wavefront group ($P<.0001$). Mean preoperative astigmatism was 2.03±0.56 D (range: 1.25 to 3.50 D) and 0.80±0.39 D (range: 0.00 to 3.50 D) for the aspheric ablation and ocular wavefront groups, respectively.

At 6 months postoperatively, mean spherical equivalent refraction was reduced to −0.13±0.18 D (range: −0.50 to +0.25 D) for the aspheric ablation group ($P<.0001$) and −0.12±0.17 D (range: −0.50 to +0.25 D) for the ocular wavefront group ($P<.0001$), with no significant differences between groups postoperatively. Mean astigmatism was reduced to 0.15±0.25 D (range: 0.00 to 0.75 D) ($P<.0005$) and 0.15±0.25 D (range: 0.00 to 0.75 D) ($P<.001$) for the aspheric ablation and ocular wavefront groups, respectively, with no significant differences between groups postoperatively. Of the eyes treated in the aspheric ablation group as well as the eyes treated in the ocular wavefront group, 91%, respectively, resulted in a postoperative astigmatism magnitude within 0.50 D. Further details can be found in the Table and Figure 7.

Corneal Aberrations

Mean preoperative RMS of the corneal higher order aberration analyzed at the 6-mm diameter was 0.33±0.15 µm (range: 0.09 to 0.87 µm) for the aspheric ablation group and 0.53±0.13 µm (range: 0.34 to 0.98 µm) for the ocular wavefront group. At 6 months postoperatively, RMS was 0.34±0.14 µm (range: 0.15 to 0.62 µm) ($P<.05$) and 0.35±0.18 D (range: 0.10 to 0.890 µm) ($P<.01$) for the aspheric ablation and ocular wavefront groups, respectively, with no significant differences between groups postoperatively. Further details can be found in Figure 8.

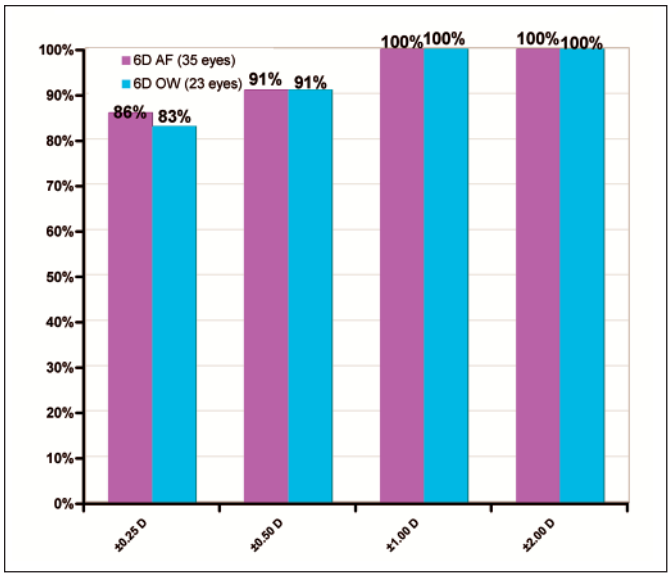

Figure 7. Refractive outcome for astigmatism in the aspheric ablation (AF) group and ocular wavefront (OW) group.

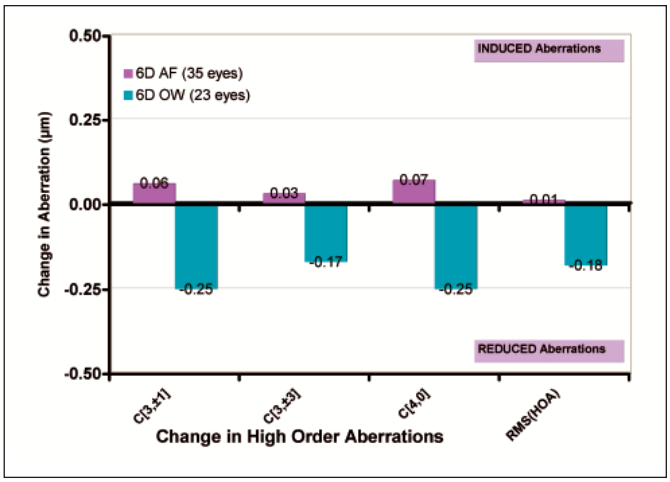

Figure 8. Change in corneal higher order aberration terms analyzed at a 6-mm diameter. Notice the minor induction of aberrations in the aspheric ablation (AF) group and the reduction in aberrations of the ocular wavefront (OW) group.

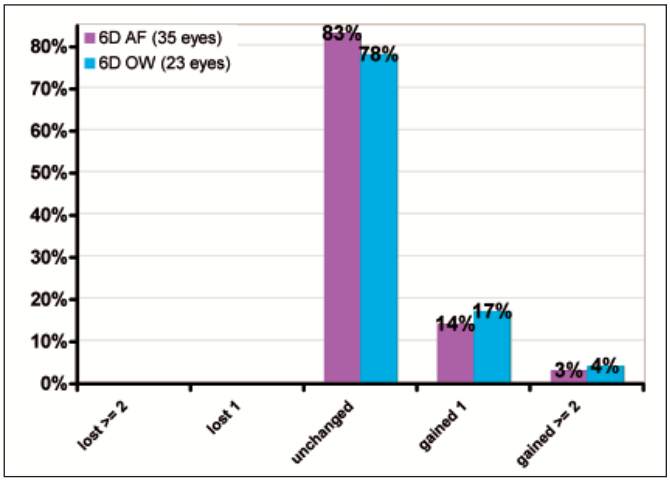

Figure 9. Distribution of the change in corrected distance visual acuity (safety) in the aspheric ablation (AF) and ocular wavefront (OW) groups.

Visual Acuity

In the aspheric ablation group, 17% of the treated eyes gained 1 or more lines of CDVA and no eye lost lines of CDVA. In the ocular wavefront group, 21% of the treated eyes gained 1 or more lines of CDVA and no eye lost lines of CDVA (Fig 9).

The mean difference in CDVA 6 months postoperatively compared to preoperative baseline was 0.2±0.4 lines (range: 0 to +2 lines) ($P<.05$) and 0.4±0.6 lines (range: 0 to +2 lines) ($P<.01$) for the aspheric ablation and ocular wavefront groups, respectively.

DISCUSSION

The methods used in this study to determine eye movements include compensation for the ocular cyclotorsions occurring from upright to supine position (static cyclotorsion from diagnosis to treatment), as well as lateral movements, eye rolling, dynamic cyclotorsion, and displacement along the propagation axis occurring during laser treatment. Furthermore, the differences in pupil size and center before and during treatment compared to that during diagnosis[35] were also compensated for, as the theoretical impact of cyclotorsional ablations is smaller than decentered ablations or edge effects[36] (coma and spherical aberration[37]). In this way, additional lateral displacements[38] due to cyclotorsions occurring around any position other than the ablation center are avoided (induced aberrations emanating from lateral displacements always increase with decentration[39]).

A 6D eye-tracker is potentially valuable because uncompensated pupil movements (lateral movements) and uncompensated rolling movements can induce decentrations,[12,15] which can visually manifest as comatic aberrations.[38] Uncompensated cyclotorsional movements may induce aberrations,[20] whereas uncompensated axial movements may induce undercorrections in an asymmetrical way. Axial movements cause the laser spots to be out of focus when they reach the cornea, ie, for the same energy spot diameter is larger, thereby reducing the radiant exposure and the ablation depth of the spot. Axial movements result in off-axis pulses hitting the cornea more centrally than planned if the eye moves towards the laser system and further peripherally if the eye moves away from the laser.

There was no a priori determinant for cooperative versus uncooperative patients. Figures 1 and 2 graphically represent the fact that eye movements vary in amplitude, velocity, and pattern.

We obtained an average of 0.15 mm of pupil displacement. The distribution of the percentage of eyes versus pupil displacement (see Fig 4) showed 13% of eyes had pupil displacements exceeding 1 mm. The ranges for pupil displacements over the treatment were relatively mild (ie, <1 mm), but with peaks of up to approximately 1.5 mm.

We obtained an average value of 5° for rolling movement. This value is actually the most commonly accepted value for "natural rolling" measured as angle alpha,[40] lambda,[41] or kappa.[42] The distribution of the percentage of eyes versus rolling movements (see Fig 6) showed 3% of eyes had rolling exceeding 8°. The ranges for the rolling movements over the treatment were found relatively mild (ie, <5°), but with peaks of up to approximately 10°.

We obtained an average cyclotorsion of 1° for static cyclotorsion, which was lower than the observations of Ciccio et al[43] who reported 4°. The distribution of the percentage of eyes versus cyclotorsional error (see Fig 4) showed 3% of eyes had cyclotorsion exceeding 8°.

Mean dynamic cyclotorsion over treatment was relatively small, but with peaks of up to approximately 5°. Considering that the average cyclotorsion resulting from the shift from the upright to the supine position is approximately ±4°,[40] it is not enough to compensate only for the static cyclotorsion without considering the dynamic cyclotorsion during the laser procedure. Finally, the effects of the dynamic cyclotorsion can be considered as optical "noise" of the applied versus the intended profiles.[44]

Without eye registration technologies,[45,46] maximum cyclotorsion measured from the shift from the upright to the supine position does not exceed ±14°,[40] which explains why "classical" spherocylindrical corrections in refractive surgery succeed without major cyclotorsional considerations. However, only limited amounts of astigmatism can effectively be corrected for this cyclotorsional error.[20]

With currently available eye registration technologies, providing an accuracy of approximately 1° and measuring static and dynamic cyclotorsion components, patients may be treated for a wider range of refractive errors with enhanced success ratios. This requires high-resolution ablation systems as well.[47,48]

With our system for measuring axial movements, we obtained an average of −300 µm. This negative value is fairly low, but indicates that patients push their heads back at the beginning of the treatment and return to a more level position during treatment (see Figs 1 and 2). The distribution of the percentage of eyes versus axial movement (see Fig 4) showed 10% of eyes had axial movements exceeding 1 mm. The ranges for axial movements over the treatment were found relatively mild, but with peaks exceeding 1 mm.

In our study, 91% of treatments resulted in a postoperative cylinder within 0.50 D, and 19% of treatments gained lines of CDVA compared to preoperative baseline ($P<.01$). In discussing visual benefits, although visual acuity data are helpful, patients with 20/20 vision may be unhappy with their visual outcomes due to poor mesopic and low contrast visual acuity; however, this was not addressed in the current study.

More clinical data are required before statements can be made regarding how much improvement can be expected from the use of this tracking technology. Of further value would be to determine if there is a benefit to patients in decreased aberrations compared to patients treated with the same laser platform without 6D tracking. Contrast sensitivity, mesopic visual acuity, and subjective patient questionnaire data would be beneficial in future studies to show whether this technology provides an appreciable difference in outcomes.

AUTHOR CONTRIBUTIONS

Study concept and design (S.A.M., M.C.A.); data collection (M.C.A.); analysis and interpretation of data (S.A.M., M.C.A.); drafting of the manuscript (S.A.M., M.C.A.); critical revision of the manuscript (M.C.A.); statistical expertise (S.A.M.)

REFERENCES

1. Munnerlyn CR, Koons SJ, Marshall J. Photorefractive keratectomy: a technique for laser refractive surgery. *J Cataract Refract Surg.* 1988;14(1):46-52.
2. Mastropasqua L, Toto L, Zuppardi E, Nubile M, Carpineto P, Di Nicola M, Ballone E. Photorefractive keratectomy with aspheric profile of ablation versus conventional photorefractive keratectomy for myopia correction: six-month controlled clinical trial. *J Cataract Refract Surg.* 2006;32(1):109-116.
3. Applegate RA, Howland HC. Refractive surgery, optical aberrations, and visual performance. *J Refract Surg.* 1997;13(3):295-299. Erratum in *J Refract Surg.* 1997;13(6):490.
4. Thibos L, Bradley A, Applegate R. Accuracy and precision of objective refraction from wavefront aberrations. *J Vis.* 2004;4(4):329-351.
5. Liang J, Grimm B, Goelz S, Bille JF. Objective measurement of wave aberrations of the human eye with the use of a Hartmann-Shack wave-front sensor. *J Opt Soc Am A Opt Image Sci Vis.* 1994;11(7):1949-1957.
6. Salmon TO. Corneal contribution to the wavefront aberration of the eye [PhD dissertation]. Bloomington, IN: Indiana University; 1999:70.
7. Mrochen M, Jankov M, Bueeler M, Seiler T. Correlation between corneal and total wavefront aberrations in myopic eyes. *J Refract Surg.* 2003;19(2):104-112.
8. Alió JL, Belda JI, Osman AA, Shalaby AM. Topography-guided laser in situ keratomileusis (TOPOLINK) to correct irregular astigmatism after previous refractive surgery. *J Refract Surg.* 2003;19(5):516-527.
9. Mrochen M, Kaemmerer M, Seiler T. Clinical results of wave-

front-guided laser in situ keratomileusis 3 months after surgery. *J Cataract Refract Surg.* 2001;27(2):201-207.

10. Mrochen M, Donetzky C, Wüllner C, Löffler J. Wavefront-optimized ablation profiles: theoretical background. *J Cataract Refract Surg.* 2004;30(4):775-785.
11. Koller T, Iseli HP, Hafezi F, Mrochen M, Seiler T. Q-factor customized ablation profile for the correction of myopic astigmatism. *J Cataract Refract Surg.* 2006;32(4):584-589.
12. Schwiegerling J, Snyder RW. Eye movement during laser in situ keratomileusis. *J Cataract Refract Surg.* 2000;26(3):345-351.
13. Taylor NM, Eikelboom RH, van Sarloos PP, Reid PG. Determining the accuracy of an eye tracking system for laser refractive surgery. *J Refract Surg.* 2000;16(5):S643-S646.
14. Bueeler M, Mrochen M, Seiler T. Maximum permissible lateral decentration in aberration-sensing and wavefront-guided corneal ablation. *J Cataract Refract Surg.* 2003;29(2):257-263.
15. Bueeler M, Mrochen M. Limitations of pupil tracking in refractive surgery: systematic error in determination of corneal locations. *J Refract Surg.* 2004;20(4):371-378.
16. Buehren T, Lee BJ, Collins MJ, Iskander DR. Ocular microfluctuations and videokeratoscopy. *Cornea.* 2002;21(4):346-351.
17. Smith EM Jr, Talamo JH, Assil KK, Petashnick DE. Comparison of astigmatic axis in the seated and supine positions. *J Refract Corneal Surg.* 1994;10(6):615-620.
18. Smith EM Jr, Talamo JH. Cyclotorsion in the seated and supine patient. *J Cataract Refract Surg.* 1995;21(4):402-403.
19. Bueeler M, Mrochen M, Seiler T. Maximum permissible torsional misalignment in aberration-sensing and wavefront-guided corneal ablation. *J Cataract Refract Surg.* 2004;30(1):17-25.
20. Arba-Mosquera S, Merayo-Lloves J, de Ortueta D. Clinical effects of pure cyclotorsional errors during refractive surgery. *Invest Ophthalmol Vis Sci.* 2008;49(11):4828-4836.
21. Chernyak DA. From wavefront device to laser: an alignment method for complete registration of the ablation to the cornea. *J Refract Surg.* 2005;21(5):463-468.
22. Chernyak DA. Cyclotorsional eye motion occurring between wavefront measurement and refractive surgery. *J Cataract Refract Surg.* 2004;30(3):633-638.
23. Bharti S, Bains HS. Active cyclotorsion error correction during LASIK for myopia and myopic astigmatism with the NIDEK EC-5000 CX III laser. *J Refract Surg.* 2007;23(9 Suppl):S1041-S1045.
24. Kim H, Joo CK. Ocular cyclotorsion according to body position and flap creation before laser in situ keratomileusis. *J Cataract Refract Surg.* 2008;34(4):557-561.
25. Park SH, Kim M, Joo CK. Measurement of pupil centroid shift and cyclotorsional displacement using iris registration. *Ophthalmologica.* 2009;223(3):166-171.
26. Porter J, Yoon G, MacRae S, Pan G, Twietmeyer T, Cox IG, Williams DR. Surgeon offsets and dynamic eye movements in laser refractive surgery. *J Cataract Refract Surg.* 2005;31(11):2058-2066. Erratum in *J Cataract Refract Surg.* 2006;32(3):378.
27. Hori-Komai Y, Sakai C, Toda I, Ito M, Yamamoto T, Tsubota K. Detection of cyclotorsional rotation during excimer laser ablation in LASIK. *J Refract Surg.* 2007;23(9):911-915.
28. Chang J. Cyclotorsion during laser in situ keratomileusis. *J Cataract Refract Surg.* 2008;34(10):1720-1726.
29. Arba Mosquera S, de Ortueta D. Analysis of optimized profiles for 'aberration-free' refractive surgery. *Ophthalmic Physiol Opt.* 2009;29(5):535-548.
30. Arbelaez MC, Vidal C, Arba Mosquera S. Clinical outcomes of LASIK for myopia using the SCHWIND platform with ocular wavefront customized ablation. *J Refract Surg.* 2009;25(12):1083-1090.
31. Arbelaez MC, Vidal C, Arba Mosquera S. Moderate-to-high astigmatism correction with the SCHWIND AMARIS Total-Tech Laser: 6-month results. *J Cataract Refract Surg.* In press.
32. Arba Mosquera S, de Ortueta D. Tissue-saving Zernike terms selection in customised treatments for refractive surgery. *J Optom.* In press.
33. Arbelaez MC, Vidal C, Arba Mosquera S. Central ablation depth and postoperative refraction in excimer laser myopic correction measured with ultrasound, Scheimpflug, and optical coherence pachymetry. *J Refract Surg.* 2009;25(8):699-708.
34. Arbelaez MC, Arba Mosquera S. The SCHWIND AMARIS Total-Tech laser as an all-rounder in refractive surgery. *Middle East Afr J Ophthalmol.* 2009;16(1):46-53.
35. Yang Y, Thompson K, Burns S. Pupil location under mesopic, photopic and pharmacologically dilated conditions. *Invest Ophthalmol Vis Sci.* 2002;43(7):2508-2512.
36. Marcos S, Barbero S, Llorente L, Merayo-Lloves J. Optical response to LASIK surgery for myopia from total and corneal aberration measurements. *Invest Ophthalmol Vis Sci.* 2001;42(13):3349-3356.
37. Marcos S. Aberrations and visual performance following standard laser vision correction. *J Refract Surg.* 2001;17(5):S596-S601.
38. Guirao A, Williams D, Cox I. Effect of rotation and translation on the expected benefit of an ideal method to correct the eye's higher-order aberrations. *J Opt Soc Am A Opt Image Sci Vis.* 2001;18(5):1003-1015.
39. Uozato H, Guyton DL. Centering corneal surgical procedures. *Am J Ophthalmol.* 1987;103(3 Pt 1):264-275. Erratum in *Am J Ophthalmol.* 1987;103(6):852.
40. Dunne MC, Misson GP, White EK, Barnes DA. Peripheral astigmatic asymmetry and angle alpha. *Ophthalmic Physiol Opt.* 1993;13(3):303-305.
41. Salmon TO, Thibos LN. Videokeratoscope-line-of-sight misalignment and its effect on measurements of corneal and internal ocular aberrations. *J Opt Soc Am A Opt Image Sci Vis.* 2002;19(4):657-669. Erratum in *J Opt Soc Am A Opt Image Sci Vis.* 2003;20(1):195.
42. Hashemi H, Khabazkhoob M, Yazdani K, Mehravaran S, Jafarzadehpur E, Fotouhi A. Distribution of angle kappa measurements with Orbscan II in a population-based survey. *J Refract Surg.* 2010;26(12):966-971.
43. Ciccio AE, Durrie DS, Stahl JE, Schwendeman F. Ocular cyclotorsion during customized laser ablation. *J Refract Surg.* 2005;21(6):S772-S774.
44. Bueeler M, Mrochen M. Simulation of eye-tracker latency, spot size, and ablation pulse depth on the correction of higher order wavefront aberrations with scanning spot laser systems. *J Refract Surg.* 2005;21(1):28-36.
45. Chernyak DA. Iris-based cyclotorsional image alignment method for wavefront registration. *IEEE Trans Biomed Eng.* 2005;52(12):2032-2040.
46. Schruender S, Fuchs H, Spasovski S, Dankert A. Intraoperative corneal topography for image registration. *J Refract Surg.* 2002;18(5):S624-S629.
47. Huang D, Arif M. Spot size and quality of scanning laser correction of higher-order wavefront aberrations. *J Cataract Refract Surg.* 2002;28(3):407-416.
48. Guirao A, Williams D, MacRae S. Effect of beam size on the expected benefit of customized laser refractive surgery. *J Refract Surg.* 2003;19(1):15-23.